Assembly-level analysis on temperature coefficient of reactivity in a graphite-moderated fuel salt reactor fueled with low-enriched uranium*

Xiao-Xiao Li,[1,2,3] De-Yang Cui,[1,2] Chun-yan Zou,[1,2,3] Jian-Hui Wu,[1,2,3] Xiang-Zhou Cai,[1,2,3,†] and Jin-Gen Chen[1,2,3,‡]

[1] *Shanghai Institute of Applied Physics, Chinese Academy of Sciences, Shanghai 201800, China*
[2] *CAS Innovative Academy in TMSR Energy System, Chinese Academy of Sciences, Shanghai 201800, China*
[3] *University of Chinese Academy of Sciences, Beijing 100049, China*

To provide a reliable and comprehensive data reference for core geometry design of graphite-moderated and low-enriched uranium fueled molten salt reactor, the influences of geometric parameters on temperature coefficient of reactivity (TCR) at an assembly level are characterized. The four-factor formula is introduced to explain how different reactivity coefficients behave in terms of fuel salt volume fraction and assembly size. The results show that fuel salt temperature coefficient (FSTC) is always negative due to a more negative fuel salt density coefficient in the over-moderated region or a more negative Doppler coefficient in the under-moderated region. Depending on the fuel salt channel spacing, the graphite moderator temperature coefficient (MTC) can be negative or positive. Further, an assembly with a smaller fuel salt channel spacing are more likely to exhibit a negative MTC. As fuel salt volume fraction increases, the negative FSTC weakens first and then increases, owing to the fuel salt density effect gradually weakening from negative feedback to positive feedback and then decreasing. Meanwhile, MTC weakens as the thermal utilization coefficient caused by the graphite temperature effect deteriorates. Thus, the negative TCR weakens first and then strengthens mainly because of the change in fuel salt density coefficient. As assembly size increases, the magnitude of FSTC decreases monotonously due to a monotonously weakened fuel salt Doppler coefficient, whereas MTC changes from gradual weakened negative feedback to gradual enhanced positive feedback. And then, the negative TCR weakens. Therefore, to achieve a proper negative TCR, particularly a negative MTC, an assembly with a smaller fuel salt channel spacing in the under-moderated region is strongly recommended.

Keywords: Molten salt reactor, Temperature coefficient of reactivity, Four-factor formula

I. INTRODUCTION

Molten salt reactor (MSR) is the only liquid-fueled reactor in the generation IV power systems [1]. Its core structure and operation mode are obviously distinct from traditional pressurized water reactor (PWR). A typical PWR uses water as coolant and moderator. As the core temperature of a PWR rises, the water density decreases and the ratio of water to uranium declines, but the fuel density remains almost constant. And PWR is usually designed in the under-moderated region to ensure a sufficiently negative moderator temperature coefficient [2]. Whereas a typical graphite-moderated MSR uses flowing fuel salt as coolant and solid graphite as moderator. As core temperature of an MSR rises, the density of graphite moderator remains essentially unchanged while the density of liquid fuel salt reduces, resulting in a higher ratio of graphite to nuclear fuel [3] and then significantly effects on temperature coefficient of reactivity (TCR). To make a reactor self-stable, it is crucial to maintain a proper negative temperature coefficient of reactivity (TCR) by adopting appropriate design parameters.

The TCR of a graphite-moderated and liquid-fueled MSR is typically divided into fuel salt temperature coefficient (FSTC) and graphite moderator temperature coefficient (MTC). FSTC is usually negative, which can be further divided into fuel salt Doppler coefficient and fuel salt density coefficient. However, MTC can be negative or positive [4], and the latter poses a potential safety risk to reactor operation. Currently, most of liquid-fueled MSRs, such as MSRE [5], MSBR [6], and FUJI [7], were all designed in the under-moderated region. Nevertheless, these designs didn't provided a systematic analysis to explain why the under-moderated region was chosen.

Some research activities have been conducted on the influencing factors of TCR in liquid-fueled MSRs, focusing on geometric parameters and fuel salt compositions. The geometric parameters [8–10] include fuel salt channel radius, fuel salt fraction, and lattice pitch, among others. The molar ratio of heavy metal (HM), the type of carrier salt, and the uranium enrichment are all important parameters associated with fuel salt compositions. The effects of fuel salt compositions on TCR for MSR have been studied using the six-factor formula [11–13]. Further research is however necessary to determine how geometric parameters affect TCR in an MSR core.

Based on a graphite-moderated and low-enriched uranium fueled MSR, this work aims to provide a more responsible contribution to variations of various reactivity coefficients with geometric parameters including fuel salt volume fraction and assembly size. This paper is organized as follows. Section II provides a brief overview of calculation model and analysis methodology. Section III discusses the behaviors of various reactivity coefficients from the perspective of the four-factor formula. Section IV contains the concluded remarks on TCR for liquid fueled MSRs.

* Supported by the Youth Innovation Promotion Association CAS (No. 2022258), the National Natural Science Foundation of China (No. 12175300), the Chinese TMSR Strategic Pioneer Science and Technology Project (No. XDA02010000) and the Young Potential Program of Shanghai Institute of Applied Physics, Chinese Academy of Sciences under Grant (No. E1550510)

† Corresponding author, caixz@sinap.ac.cn
‡ Corresponding author, chenjg@sinap.ac.cn

II. CALCULATION MODEL AND ANALYSIS METHODOLOGY

A. Calculation model

A graphite-moderated fuel salt assembly includes two regions (Figure 1): a central circular region filled with fuel salt (defined as fuel salt channel) and a hexagonal outer region composed of graphite moderator. The assembly geometry can be characterized by the side length of assembly (L), the opposite side distance (P), the radius of fuel salt channel (R), and the fuel salt channel spacing (D) representing the distance between two adjacent fuel salt channels' outer margins. It should be noted that the maximum fuel salt volume fraction (VF) is set to 50%. This is primarily because there is almost no Maxwell spectrum and MTC approaches zero when the fuel salt volume fraction exceeds 50%.

The adopted fuel salt composition in this work is LiF-BeF_2-UF_4 (68-20-12 mole%). Previous studies have revealed more detailed analyses on the effect of the concentration of heavy metal on TCR [11, 12], which will not be discussed in this work. To reduce harmful neutron absorption of Li-6, the abundance of Li-7 is set to 99.995%. Low enriched uranium (<20% U-235 enrichment)) is used in this study for nonproliferation and availability.

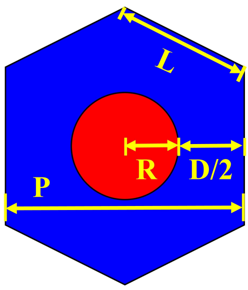

Fig. 1. Schematic of a graphite-moderated fuel salt assembly.

B. Analysis methodology

This study was conducted for a single graphite-moderated fuel salt assembly that was infinitely reflected in both the radial and axial directions. In this case, the moderator is graphite, and the nuclear fuel is melted in the carrier salt [14], which includes F, Li, and Be, exhibits certain moderating properties. The Four-factor formula for an infinite medium [15], $k_{\rm inf}=\varepsilon p \eta f$, is used to qualitatively understand the mechanisms of TCR of an MSR at assembly level. Here, ε, p, η and f represent the fast fission factor, the resonance escape probability, the thermal reproduction factor, and the thermal utilization factor, respectively. The four factors and their corresponding reactivity coefficients for a graphite-moderated fuel salt assembly with low enriched uranium are detailed as follows. It is crucial to keep in mind that the nuclear fuels (or heavy metals) are integrated into the fuel salt, the fission or absorption contributions of them should be subtracted from the fuel salt when calculating the four factors, especially for the fast fission factor and the thermal reproduction factor.

The fast fission factor, $\varepsilon = F_{\rm t}^{\rm HM}/F_1^{\rm HM}$, is defined as the ratio of the number of neutrons produced by fissions at all energies (total production) to that produced by thermal fission (thermal production). The thermal reproduction factor, $\eta = F_1^{\rm HM}/A_1^{\rm HM}$, is the ratio of the number of neutrons produced by thermal fission (thermal production) to that of thermal neutrons absorbed in nuclear fuel (thermal absorption). Here, $F_{\rm t}$, F_1 and A_1 represent the total production, the thermal production and the thermal absorption, respectively. Since fast fission occurs primarily in U-238 but also in U-235 when low enriched uranium is used, the subscript "HM" includes U-235 and U-238.

The resonance escape probability, $p = A_1^{\rm tot}/A_t^{\rm tot} = A_1^{\rm salt} + A_1^{\rm gra}$, is described as the ratio of neutrons reaching thermal energies to fast neutrons slowing down. The thermal utilization factor, $f = A_1^{\rm HM}/A_1^{\rm tot} = A_1^{\rm HM}/(A_1^{\rm HM} + A_1^{\rm FLiBe} + A_1^{\rm gra}) = A_1^{\rm HM}/(A_1^{\rm HM} + A_1^{\rm FLiBe,gra})$, is represented as the ratio of thermal neutrons absorbed in heavy metal to those absorbed in all the materials in the assembly. Here, A_t represents the total absorption and $A_t^{\rm tot}$ equals 1.0. The superscripts "HM", "FLiBe", "gra" and "tot" represent the thermal absorption of heavy metal, carrier salt, graphite and all the materials in the assembly, respectively.

The temperature coefficient of reactivity, $\alpha_{\rm T}$, defined as the change in reactivity caused by the change in temperature of all the materials in the assembly [16], is expressed by Eq. (1) when $k_{\rm inf}$ approaches 1.0. Temperature (T) rises in 100 K increments from 780 K to 1080 K considering the melting point of the fuel salt and the possible temperature range of MSR.

$$\alpha_{\rm T} = \frac{1}{k_{\rm inf}} \frac{{\rm d}k_{\rm inf}}{{\rm d}T} \tag{1}$$

According to Eq. (2), each TCR can be decomposed into four reactivity coefficients [17], including fast fission coefficient ($\alpha_{\rm T}^{\varepsilon}$), resonance escape coefficient ($\alpha_{\rm T}^{p}$), thermal reproduction coefficient ($\alpha_{\rm T}^{\eta}$), and thermal utilization coefficient ($\alpha_{\rm T}^{f}$).

$$\alpha_{\rm T} = \alpha_{\rm T}^{\varepsilon} + \alpha_{\rm T}^{p} + \alpha_{\rm T}^{\eta} + \alpha_{\rm T}^{f} \tag{2}$$

Eqs. (3)∼ (6) presents the calculation methods for four reactivity coefficients. Here, "d" denotes the absolute change in parameter caused by temperature change and "Δ" denotes the rate at which the parameter changes with temperature.

$$\alpha_{\rm T}^{\varepsilon} = \frac{1}{\varepsilon}\frac{{\rm d}\varepsilon}{{\rm d}T} = \Delta F_{\rm t}^{\rm HM} - \Delta F_1^{\rm HM} = \frac{1}{F_{\rm t}^{\rm HM}}\frac{{\rm d}F_{\rm t}^{\rm HM}}{{\rm d}T} - \frac{1}{F_1^{\rm HM}}\frac{{\rm d}F_1^{\rm HM}}{{\rm d}T} \tag{3}$$

$$\alpha_{\rm T}^{p} = \frac{1}{p}\frac{{\rm d}p}{{\rm d}T} = \Delta A_1^{\rm salt} + \Delta A_1^{\rm gra} = \frac{1}{A_1^{\rm salt} + A_1^{\rm gra}}\left(\frac{{\rm d}A_1^{\rm salt}}{{\rm d}T} + \frac{{\rm d}A_1^{\rm gra}}{{\rm d}T}\right) \tag{4}$$

$$\alpha_{\rm T}^{\eta} = \frac{1}{\eta}\frac{{\rm d}\eta}{{\rm d}T} = \Delta F_1^{\rm HM} - \Delta A_1^{\rm HM} = \frac{1}{F_1^{\rm HM}}\frac{{\rm d}F_1^{\rm HM}}{{\rm d}T} - \frac{1}{A_1^{\rm HM}}\frac{{\rm d}A_1^{\rm HM}}{{\rm d}T} \tag{5}$$

$$\alpha_{\mathrm{T}}^{f} = \frac{1}{f}\frac{\mathrm{d}f}{\mathrm{d}T} = \Delta A_1^{\mathrm{HM}} - \Delta A_1^{\mathrm{FLiBe,gra}} = \frac{A_1^{\mathrm{FLiBe,gra}}}{A_1^{\mathrm{tot}}}\left(\frac{1}{A_1^{\mathrm{HM}}}\frac{\mathrm{d}A_1^{\mathrm{HM}}}{\mathrm{d}T} - \frac{1}{A_1^{\mathrm{FLiBe,gra}}}\frac{\mathrm{d}A_1^{\mathrm{FLiBe,gra}}}{\mathrm{d}T}\right) \quad (6)$$

It's important to note that U-235 plays a dominate role in feedback, particularly for $\alpha_{\mathrm{T}}^{\varepsilon}$ and $\alpha_{\mathrm{T}}^{\eta}$, because its microscopic cross section is significantly higher than that of U-238 over the thermal energy region, particularly when neutron energy is less than 0.1 eV. Therefore, in the following discussions, we will focus on U-235's contribution to the fast fission coefficient ($\alpha_{\mathrm{T}}^{\varepsilon}$) and the thermal reproduction coefficient ($\alpha_{\mathrm{T}}^{\eta}$).

MCNP5 handles neutronic calculations such as criticality and reactivity coefficients. The FMn tally multiplier card is used to calculate cross sections and factors in the four-factor formula. To perform accurate calculations with uranium-based fuel, a compact ENDF (ACE) format cross section library with continuous energy was chosen based on the ENDF/B-VII library. In order to increase computational accuracy and efficiency, each criticality calculation is excused to skip 50 cycles and run a total of 1050 cycles with 100,000 neutrons per cycle. The maximum computing time for one criticality calculation using 12 processors is less than 36 hours. The estimated standard deviation of k_{inf} is about 5 pcm.

III. RESULTS AND DISCUSSIONS

A. Critical parameters

Considering the characteristics of online refueling and reprocessing for a liquid-fueled MSR, the initial excess reactivity of a graphite-moderated fuel salt assembly can be set low (k_{inf} =1.02∼1.03). And then, the required critical enrichment of U-235 is searched by varying assembly size (L) from 3.0 cm to 24.0 cm and fuel salt volume fraction (VF) from 1% to 50%. The fuel salt channel spacing is closely related to the required critical enrichment of U-235 and the temperature coefficient of reactivity, and its variation with fuel salt volume fraction and assembly size is shown in Figure 2 (a). Increasing fuel salt volume fraction and decreasing assembly size can result in a decrease in fuel salt channel spacing. Meanwhile, the larger the assembly size, the faster fuel salt channel spacing decreases with increasing fuel salt volume fraction.

The variations of the infinite multiplication factor at a fixed U-235 enrichment (19.75 wt%) and the required critical enrichment of U-235 with fuel salt volume fraction and assembly size are given in Figure 2 (b) and Figure 2 (c), respectively. When fuel salt volume fraction is raised for a fixed assembly size, the neutron spectrum hardens, and the residence time of neutrons in high energy region of fast fission is prolonged. Hence, the fast neutron multiplication effect is enhanced, and the fast fission factor increases. Meanwhile, as graphite moderator volume fraction decreases, the ratio of graphite to heavy metal declines, and the probability of neutrons being absorbed by nuclear fuel or moderator in

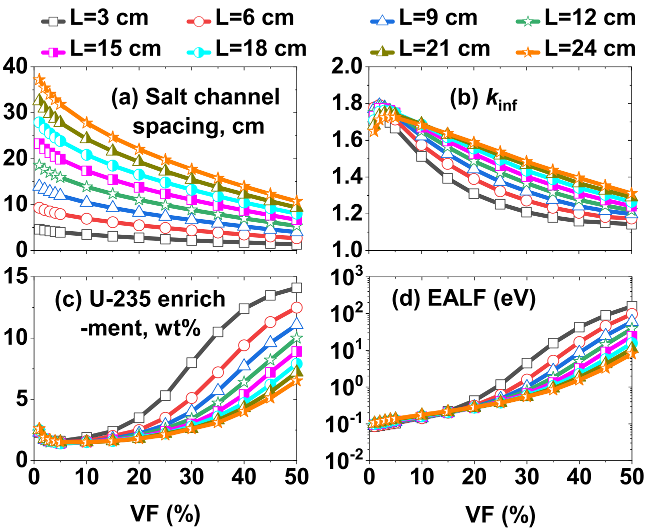

Fig. 2. Variations of fuel salt channel spacing (a), k_{inf} (b), critical enrichment of U-235 (c) and EALF (d) with fuel salt volume fraction for different assembly sizes.

epi-thermal neutron energy region increases, making it more difficult for neutrons to escape from resonance region, and thus the resonance escape probability decreases. The thermal reproduction factor, on the other hand, varies only slightly with fuel salt volume fraction, with a maximum variation of less than 0.6%. As the ratio of fuel salt volume to graphite volume further increases, the thermal absorption of fuel salt exceeds that of graphite, and the thermal utilization factor rises. Based on the variations of four factors, the infinite multiplication factor first increases corresponding to the under-moderated region and then decreases corresponding to the over-moderated region as fuel salt volume fraction increases. On the contrary, the required critical enrichment of U-235 decreases in the over-moderated region and then increases in the under-moderated region.

For a constant fuel salt volume fraction, as assembly size increases, the graphite through which the incident neutrons thickens, neutrons can be slowed down even better, neutron spectrum softens. In this case, the fast neutron multiplication effect weakens, and the fast fission factor decreases. Meanwhile, the absorption probability of resonance neutrons generated in graphite by heavy metal decreases, resulting in an increase in resonance escape probability [18]. The thermal reproduction factor is also not visibly affected by the assembly size, with a maximum variation of less than 0.4%. As fuel salt channel spacing increases with increasing assembly size, the thermal neutron absorption of nuclear fuel decreases while that of graphite moderator increases, and then the thermal utilization factor decreases. As assembly size increases, a slight decrement in the infinite multiplication factor and a slight increment in the required critical enrichment of U-235 are displayed in the over-moderated region. Meanwhile, the infinite multiplication factor rises while the required critical enrichment of U-235 falls in the under-moderated region.

Neutron spectrum is essential for determining the influ-

ence factors of TCR. To quantitatively characterize the neutron spectrum in a reactor, a spectrum factor defined as the energy corresponding to the average neutron lethargy causing fission (EALF) [12] is introduced and its variation with fuel salt volume fraction and assembly size is displayed in Figure 2 (d). As fuel salt volume fraction increases for a constant assembly size, the required critical enrichment of U-235 increases especially in the under-moderated region, allowing for more production of fast neutrons. As fuel salt channel spacing decreases, the fast neutrons released from fuel salt cannot be fully moderated. These two factors harden neutron spectrum, leading to an increase in EALF. The effect of assembly size on EALF is associated with the moderated region. First, when the assembly tends to the over-moderated region, the graphite parasitic absorption becomes stronger, the likelihood of fast neutrons being slowed down to thermal neutrons decreases. And, a slightly increasing required critical enrichment of U-235 results in more fast neutron generation as assembly size increases. Thus, neutron spectrum hardens and EALF increases as assembly size increases in the over-moderated region. Second, when the assembly tends to the under-moderated region, the graphite dominates the scattering reaction. As assembly size increases, the likelihood of fast neutrons colliding with graphite nuclide increases, as does the possibility of fast neutrons being slowed down into thermal neutrons. At the same time, an increasing assembly size causes a decrease in the required critical enrichment of U-235 and less fast neutron generation. Thus, neutron spectrum softens and EALF decreases as assembly size increases in the under-moderated region.

B. Fuel salt Doppler coefficient

The Doppler effect, which can be used to explain the Doppler broadening of the resonance capture cross-sections of nuclear fuel since it determines the fuel salt temperature coefficient. From the point of view of the four-factor formula, the fuel salt Doppler coefficient can be decomposed into four reactivity coefficients, i.e., fast fission coefficient, resonance escape coefficient, thermal reproduction coefficient, and thermal utilization coefficient, as demonstrated in Eq. (2). Their variations with fuel salt volume fraction and assembly size are presented in Figure 3.

The Doppler broadening of resonance caused by an increase in fuel salt temperature leads to a hardening neutron spectrum, which causes the residence time of neutrons in high energy region of fast fission to be longer, the fast neutron multiplication effect to be enhanced, and the fast fission factor increases. Thus, the fast fission coefficient in Doppler coefficient, $\alpha_{\mathrm{T}}^{\varepsilon}(\mathrm{dop})$, is positive. Its magnitude is primarily determined by the difference between U-235's thermal production and U-235's total production, and it is very closely related to the change of neutron spectrum. When fuel salt volume fraction or assembly size changes, if neutron spectrum becomes harder and EALF increases, which means that the proportion of U-235's thermal production in U-235's total production decreases, and then the gap between the variations in U-235's total production and U-235's thermal production becomes wider. It implies that the magnitude of fast fission coefficient in Doppler coefficient grows. By contrary, when neutron spectrum softens, the magnitude of fast fission coefficient in Doppler coefficient decreases. As a result, Figure 3 (a) shows that for a constant assembly size, the magnitude of fast fission coefficient in Doppler coefficient increases monotonously as fuel salt volume fraction increases. As assembly size increases for a fixed fuel salt volume fraction, the

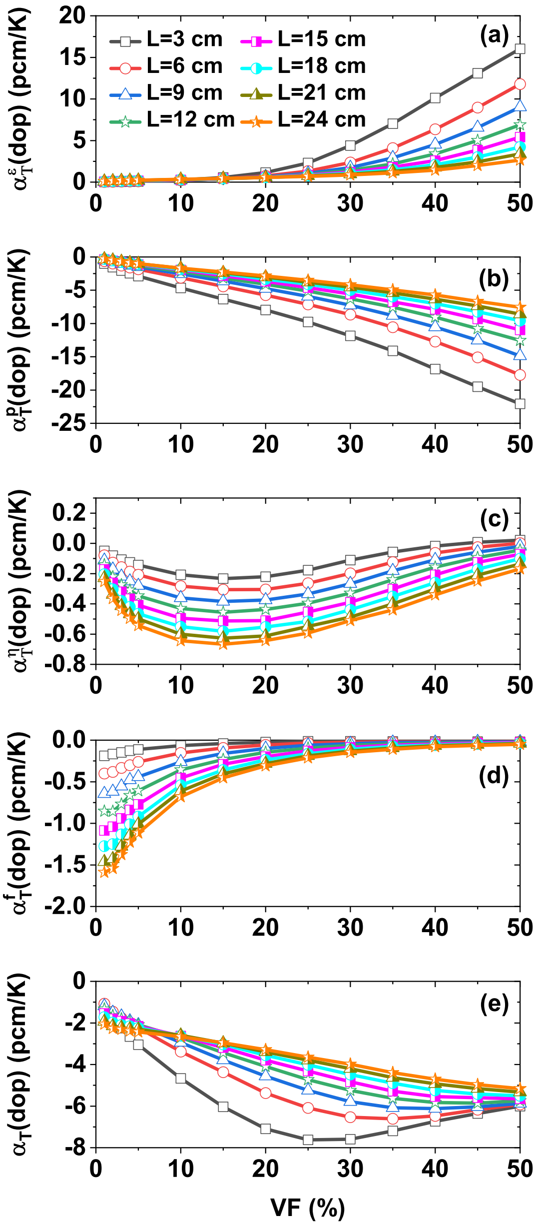

Fig. 3. Variations of different reactivity coefficients caused by the Doppler effect with fuel salt volume fraction and assembly size. (a) $\alpha_{\mathrm{T}}^{\varepsilon}(\mathrm{dop})$: fast fission coefficient in Doppler coefficient; (b) $\alpha_{\mathrm{T}}^{p}(\mathrm{dop})$: resonance escape coefficient in Doppler coefficient; (c) $\alpha_{\mathrm{T}}^{\eta}(\mathrm{dop})$: thermal reproduction coefficient in Doppler coefficient; (d) $\alpha_{\mathrm{T}}^{f}(\mathrm{dop})$: thermal utilization coefficient in Doppler coefficient; and (e) $\alpha_{\mathrm{T}}(\mathrm{dop})$: Doppler coefficient.

magnitude of fast fission coefficient in Doppler coefficient increases slightly in the over-moderated region but significantly decreases in the under-moderated region. Overall, the magnitude of fast fission coefficient in Doppler coefficient is positively correlated with EALF.

When fuel salt temperature rises, the Doppler broadening effect enhances the resonance absorption of nuclear fuel and lowers the likelihood of neutrons passing through the epithermal region to thermal region, the thermal absorption of fuel salt decreases. Nevertheless, the thermal absorption of graphite may decrease for a smaller fuel salt channel spacing or may increase for a larger fuel salt channel spacing. This is because the thermal neutrons generated mainly in graphite have higher probability to be absorbed by graphite itself when fuel salt channel spacing is relatively large. Since the Doppler effect mainly affects the heavy metals in fuel salt, the change in thermal absorption of fuel salt is usually at least one order of magnitude greater than the change in thermal absorption of graphite. Thus, the sum of changes in thermal absorptions of fuel salt and graphite is always negative. And consequently, the resonance escape coefficient in Doppler coefficient, α_{T}^{p}(dop), is negative. From Figure 3 (b), it can be concluded that the variation of resonance escape coefficient in Doppler coefficient comes mainly from the sum of the thermal absorptions of fuel salt and graphite, and to a lesser degree, from their changes. That is, for a constant assembly size, as fuel salt volume fraction increases, a harder neutron spectrum makes the sum of the thermal absorptions of fuel salt and graphite lower. Hence, a larger variation in resonance escape probability is revealed, and a stronger resonance escape coefficient in Doppler coefficient is presented for a larger fuel salt volume fraction corresponding to a smaller fuel salt channel spacing. As assembly size increases for a fixed fuel salt volume fraction, the fuel salt channel spacing widens, the sum of the thermal absorptions of fuel salt and graphite gradual increases, weakening the resonance escape coefficient in Doppler coefficient.

The Doppler broadening effect hardens neutron spectrum, increasing the resonance absorption of nuclear fuel and decreasing the probability of thermal neutrons being absorbed by nuclear fuel. Both U-235's thermal production and U-235's total absorption decrease. Since the microscopic fission cross section of U-235 is greater than its microscopic capture cross section, especially in thermal neutron region, and the average number of fission neutrons of U-235 is generally greater than 2.0, the absolute decrement of thermal production is always stronger than that of thermal absorption. For most combinations of fuel salt volume fraction and assembly size, despite the fact that U-235's thermal production is larger than U-235's thermal absorption, the absolute variation in U-235's thermal production is still larger than that in U-235's thermal absorption, and then the thermal reproduction factor decreases and further leads to a negative thermal reproduction coefficient in Doppler coefficient ($\alpha_{\mathrm{T}}^{\eta}$(dop)). However, for an assembly with a very small fuel salt channel spacing (e.g., L=3 cm and VF =40%), the graphite thickness that neutrons passes is relatively small, neutrons are not sufficiently slowed down, the probability of thermal neutron production is reduced, as does U-235's absorption (both fission and capture). In this case, the difference between U-235's thermal production and its thermal absorption is greater than the difference between the decrement of U-235's thermal production and that of U-235's thermal absorption. Thus, the variation in U-235's thermal production has a lower absolute value than the variation in U-235's thermal absorption, increasing the thermal reproduction factor and causing a positive thermal reproduction coefficient in Doppler coefficient. It can be concluded from Figure 3 (c) that the magnitude of thermal reproduction coefficient in Doppler coefficient increases first and then decreases as fuel salt volume fraction increases but increases monotonously with increasing assembly size. First, as fuel salt volume fraction increases, a hardening neutron spectrum causes decrements in both U-235's thermal production and its thermal absorption, followed by increments in both the variation in U-235's thermal production and that in U-235's thermal absorption. When fuel salt volume fraction begins to rise, the proportion of thermal neutrons is relatively high, the increase of the variation in U-235's thermal production is greater than that in U-235's thermal absorption, causing the magnitude of thermal reproduction coefficient in Doppler coefficient to increase slightly. However, as fuel salt volume fraction continues to increase, the share of thermal neutron absorption decreases while the share of resonance neutron absorption and fast neutron absorption increases. At this point, the increase of the variation in U-235's thermal absorption gradually exceeds that in U-235's thermal production, causing the magnitude of thermal reproduction coefficient in Doppler coefficient to decrease. And the negative thermal reproduction coefficient in Doppler coefficient strengths first and then weakens as fuel salt volume fraction increases for a constant assembly size. Second, the change in thermal reproduction coefficient in Doppler coefficient with assembly size is divided into two phases according to fuel salt volume fraction. When fuel salt volume fraction is very small (e.g., VF=1%) or very large (e.g., VF=40%), the absolute changes of U-235's thermal production and U-235's thermal absorption increase with increasing assembly size, but the former increases faster than the latter. As a result, the increment of the variation in U-235's thermal production is greater than that in U-235's thermal absorption, the magnitude of thermal reproduction coefficient in Doppler coefficient increases as assembly size increases. When fuel salt volume fraction is close to the optimal moderated zone (e.g., VF=15%), an increasing resonance absorption share causes the absolute changes of U-235's thermal production and that of U-235's thermal absorption to decrease with increasing assembly size, with the latter decreasing faster than the former. And then, the decrease of the variation in U-235's thermal absorption is greater than that in U-235's thermal production, the magnitude of thermal reproduction coefficient in Doppler coefficient is still increasing as assembly size increases. Therefore, when fuel salt volume fraction is constant, the magnitude of thermal reproduction coefficient in Doppler coefficient increases monotonously with increasing assembly size. It should be noted that the magnitudes of thermal reproduction coefficient in Doppler coefficient for all combinations

of fuel salt volume fraction and assembly size are quite small ($<$ 0.7 pcm/K).

The thermal absorption of fuel salt decreases as fuel salt temperature rises owing to a hardening neutron spectrum caused by the Doppler effect. After that, the thermal absorptions of heavy metal and carrier salt decrease. The variation in thermal absorption of graphite is related to the fuel salt channel spacing. First, for assembly with a smaller fuel salt channel spacing, the thermal absorption of graphite is primarily affected by the hardening neutron spectrum, and the thermal absorption of graphite decreases, as does the sum of thermal absorptions of carrier salt and graphite. Second, as fuel salt channel spacing increases, neutrons have more chances of colliding with graphite nuclei, the probability of neutrons slowing down into thermal neutrons increases, and the thermal absorption of graphite increases. In this case, the sum of the thermal absorptions of carrier salt and graphite may increase in the over-moderated region or decrease in the under-moderated region. In either case, however, the change in thermal absorption of heavy metal is always stronger than that in the sum of thermal absorptions of carrier salt and graphite caused by the Doppler effect, resulting in a decrease in thermal utilization factor and a negative thermal utilization coefficient in Doppler coefficient (α_{T}^{f}(dop)). The magnitude of thermal utilization coefficient in Doppler coefficient is primarily related to the ratio of the sum of the thermal absorptions of carrier salt and graphite to the thermal absorptions of all materials according to Eq. 6. From Figure 3 (d), for a fixed assembly size, as fuel salt volume fraction increases, fuel salt channel spacing decreases, the graphite volume fraction decreases, and the ratio of the sum of the thermal absorptions of carrier salt and graphite to the thermal absorptions of all materials is less than 1.0 and becomes smaller, while the negative thermal utilization coefficient in Doppler coefficient weakens. Meanwhile, for a constant fuel salt volume fraction, as assembly size increases, the graphite thickness through which neutrons passed between two collisions with nuclear fuel increases, implying that more thermal neutrons may be absorbed by graphite. Then, the ratio of the sum of the thermal absorptions of carrier salt and graphite to the thermal absorptions of all materials grows larger and larger, and the negative thermal utilization coefficient in Doppler coefficient strengths. To summarize, the negative thermal utilization coefficient in Doppler coefficient is proportional to fuel salt channel spacing.

Figure 3 (e) depicts the variation of Doppler coefficient with fuel salt volume fraction and assembly size. The behavior of Doppler coefficient is primarily governed by the variations of fast fission coefficient, resonance escape coefficient, and thermal utilization coefficient. Because the sum of the negative resonance escape coefficient and the negative thermal utilization coefficient is always greater than the positive fast fission coefficient, the Doppler coefficient is always negative. The magnitude of Doppler coefficient varies with fuel salt volume fraction, mainly depending on the competition between fast fission coefficient and resonance escape coefficient. Increasing fuel salt volume fraction increases the magnitude of Doppler coefficient firstly due mainly to an enhancement in resonance escape coefficient, and it reaches a maximum negative value before beginning to decrease with further increases in fuel salt volume fraction due to an enhancing positive fast fission coefficient. As assembly size increases, the magnitude of fuel salt Doppler coefficient increases in the over-moderated region due to a slight enhancement in thermal utilization coefficient and decreases in the under-moderated region due to a gradually weakened resonance escape coefficient.

C. Fuel salt density coefficient

The fuel salt density effect occurs because a small amount of fuel salt is ejected from the reactor core as its density decreases with increasing fuel salt temperature. The decrease in fuel salt density results in two major effects: the first is an increase in collision probability between fast neutron and graphite nuclei as a result of the reduced collision probability between fast neutron and nuclear fuel, and the second is a reduction in resonance absorption of nuclear fuel, which results in more fast neutrons being slowed down to thermal neutrons. Both effects can soften neutron spectrum and influence fuel salt density coefficient. Similar to fuel salt Doppler coefficient, fuel salt density coefficient can also be divided into four parts, namely fast fission coefficient, resonance escape coefficient, thermal reproduction coefficient, and thermal utilization coefficient caused by the fuel salt density effect. The variations of fuel salt density coefficient and its four reactivity coefficients are presented in Figure 4.

When fuel salt temperature increases, a softening neutron spectrum caused by the fuel salt density effect weakens the fast neutron multiplication effect, and then the fast fission factor reduces. Thus, the fast fission coefficient in density coefficient, $\alpha_{\mathrm{T}}^{\varepsilon}$(den), is negative. The variation of fast fission coefficient in density coefficient with fuel salt volume fraction and assembly size is similar to that in Doppler coefficient, and it is primarily determined by the shift of neutron spectrum. As shown in Figure 4 (a), for a constant assembly size, as fuel salt volume fraction increases, neutron spectrum hardens, the proportion of thermal production in total production for U-235 decreases, the gap between the variation in U-235's total production and that in U-235's thermal production enlarges, and then the fast fission coefficient in density coefficient is enhanced. Similarly, as assembly size increases, the magnitude of fast fission coefficient in density coefficient either increases because of a gradual hardening neutron spectrum in the over-moderated region or decreases because of a gradual softening neutron spectrum in the under-moderated region. In general, the magnitude of fast fission coefficient in density coefficient is positively correlated with EALF.

As fuel salt temperature rises, a softening neutron spectrum caused by the fuel salt density effect increases the thermal absorption of graphite. The change in thermal absorption of fuel salt is influenced by both density reduction and spectrum softening, which is closely related to the moderated region. In the over-moderated region, the change in thermal absorption of fuel salt is due mainly to a decrease in fuel salt density, result-

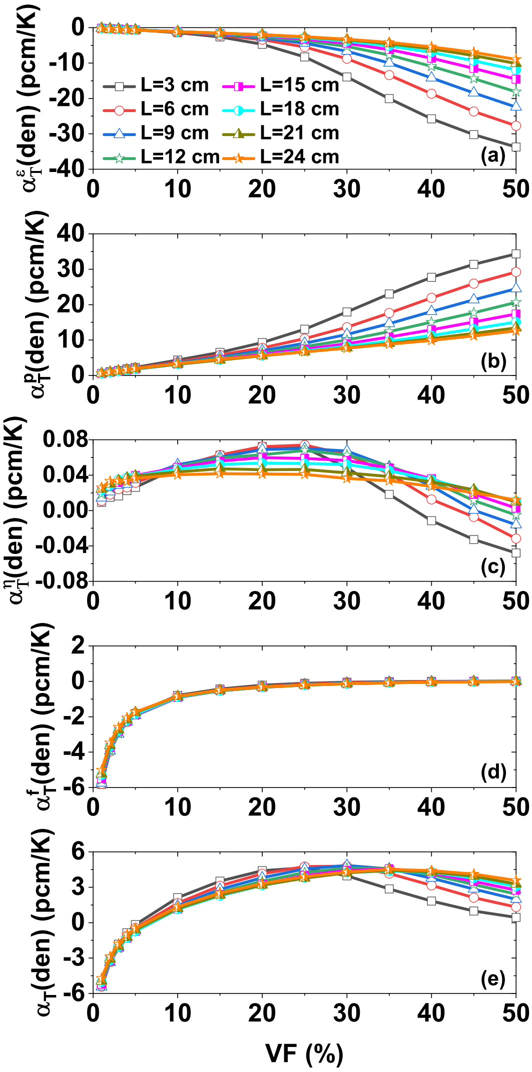

Fig. 4. Variations of different reactivity coefficients caused by the fuel salt density effect with fuel salt volume fraction and assembly size. (a) $\alpha_{\mathrm{T}}^{\varepsilon}$(den): fast fission coefficient in density coefficient; (b) α_{T}^{p}(den): resonance escape coefficient in density coefficient; (c) $\alpha_{\mathrm{T}}^{\eta}$(den): thermal reproduction coefficient in density coefficient; (d) α_{T}^{f}(den): thermal utilization coefficient in density coefficient; and (e) α_{T}(den): density coefficient.

ing in a numerical decrease. In this case, a lower fuel salt volume fraction corresponds to a higher graphite volume share, and the decrease of thermal absorption of fuel salt is smaller than the increase of thermal absorption of graphite. Thus, the sum of thermal absorptions of fuel salt and graphite is positive. In the under-moderated region, the change of thermal absorption of fuel salt is primarily due to a softening neutron spectrum, and its value will increase, as does the sum of the thermal absorptions of fuel salt and graphite. The resonance escape probability increases in either case, and the resonance escape coefficient in density coefficient, α_{T}^{p}(den), is positive. From Figure 4 (b), the magnitude of resonance escape coefficient in density coefficient is also associated with fuel salt channel spacing, and its variation with fuel salt volume fraction and assembly size is also determined by the sum of the thermal absorptions of fuel salt and graphite. As fuel salt volume fraction increases or assembly size decreases, the sum of thermal absorptions of fuel salt and graphite increases, as does the magnitude of resonance escape coefficient in density coefficient. In short, the magnitude of resonance escape coefficient in density coefficient is inversely related to the fuel salt channel spacing.

The fuel salt density effect causes a decrease in fuel salt density and then a softening neutron spectrum as fuel salt temperature increases. These two variables can determine whether the thermal reproduction coefficient in density coefficient, $\alpha_{\mathrm{T}}^{\eta}$(den), is positive or negative. First, the density reduction is usually reflected in the region with a relatively soft neutron spectrum (such as VF=1%). In this case, even though the decrement of U-235's thermal production is greater than that of U-235's thermal absorption, the decrement of the variation in U-235's thermal production is smaller than that in U-235's thermal absorption due to the fact that U-235's thermal production is much greater than U-235's thermal absorption, and then a positive thermal reproduction coefficient in density coefficient is presented. Second, a softening neutron spectrum causes increases of both U-235's thermal production and U-235's thermal absorption, but the former is faster than the latter. The increase in the variation in U-235's thermal production and that in U-235's thermal absorption in this case is closely related to the fuel salt channel spacing. For a larger fuel salt channel spacing, the difference between U-235's thermal production and U-235's thermal absorption has no effect on the gap between the increment of U-235's thermal production and that of U-235's thermal production, and then the increment in the variation in U-235's thermal production is still greater than that in U-235's thermal absorption, resulting in a positive thermal reproduction coefficient in density coefficient. For a smaller fuel salt channel spacing, the difference between U-235's thermal production and U-235's thermal absorption is greater than the difference between their respective increments, and then the increment in the variation in U-235's thermal production is smaller than that in U-235's thermal absorption, revealing a negative thermal reproduction coefficient in density coefficient. With increasing fuel salt volume fraction, the positive thermal reproduction coefficient caused by the density reduction effect gradually turns to the positive thermal reproduction coefficient caused by the spectrum softening effect. Therefore, a negative feedback is attained. Figure 4 (c) shows that with increasing fuel salt volume fraction, the positive thermal reproduction coefficient in density coefficient firstly strengths, then weakens and becomes negative. The variation of thermal reproduction coefficient in density coefficient with assembly size is related to the moderated region. There is no significant difference in thermal reproduction coefficient in density coefficient between different assembly sizes in the over-moderated region. An increasing assembly size in the under-moderated region results in a weakening negative feedback or a strengthening positive feedback. When assembly is near the optimal moderated region, the positive feedback caused by the softening spectrum effect gradually weakens as assembly

size increases. Overall, the thermal reproduction coefficient in density coefficient contributes very little ($<$ 0.1 pcm/K) to fuel salt density coefficient.

As fuel salt temperature rises, its density decreases and neutron spectrum softens. Graphite's thermal absorption increases due to a softening neutron spectrum, and then the thermal absorption of graphite grows larger. The moderated regions affect the change in thermal absorption of fuel salt. In the over-moderated region, the thermal absorption of fuel salt decreases mainly due to a reduction of fuel salt density, as will the thermal absorption of heavy metal and that of carrier salt. In this case, because the increase in thermal absorption of graphite is greater than the decrease in thermal absorption of carrier salt as a result of a larger graphite volume fraction, the sum of thermal absorptions of graphite and carrier salt shows an increase effect, and then the thermal utilization factor decreases. In the under-moderated region, the thermal absorption of heavy metal and that of carrier salt increase mainly due to a softening neutron spectrum, but the reduction in fuel salt density attenuates the increase rate of thermal absorption of heavy metal. Since the increase in thermal absorption of heavy metal is less than that in the sum of the thermal absorptions of carrier salt and graphite, the thermal utilization factor decreases. In any case, the thermal utilization coefficient in density coefficient, α_{T}^{f}(den), is always negative (Figure 4 (d)). Similarly, the magnitude of thermal utilization coefficient in density coefficient is closely related to the ratio of the sum of the thermal absorptions of carrier salt and graphite to the thermal absorptions of all materials. As fuel salt volume fraction increases for a constant assembly size, the ratio of the sum of the thermal absorptions of carrier salt and graphite to the thermal absorptions of all materials gradually decreases with a decreasing graphite volume fraction, and then the negative thermal utilization coefficient in density coefficient weakens. At a fixed fuel salt volume fraction, the difference in thermal utilization coefficient in density coefficient for different assembly sizes can be negligible.

The change in fuel salt density coefficient with fuel salt volume fraction and assembly size is depicted in Figure 4 (e). Because the magnitude of thermal reproduction coefficient is very small, the feedback and the magnitude of density coefficient vary with fuel salt volume fraction and assembly size, owing primarily to variations in fast fission coefficient, resonance escape coefficient, and thermal utilization coefficient. First, in the over-moderated region, because the feedbacks of fast fission coefficient and resonance escape coefficient are opposite and their magnitudes are close, the density coefficient exhibits a negative feedback due to a more negative thermal utilization coefficient. Second, in the under-moderated region, the magnitude of thermal utilization coefficient is small in comparison to the magnitudes of fast fission coefficient and resonance escape coefficient, and the feedback and the magnitude of density coefficient are primarily determined by the latter two. Because the negative fast fission coefficient is weaker than the positive resonance escape coefficient in this case, the feedback of density coefficient is positive. Finally, the density coefficient is more sensitive to fuel salt volume fraction rather than assembly size. With increasing fuel salt volume fraction, the negative density coefficient decreases firstly due to a decreasing thermal utilization coefficient, then turns into an increasing positive density coefficient due to an increasing positive resonance escape coefficient, and finally the positive density coefficient decreases due to an increasing negative fast fission coefficient.

D. Fuel salt temperature coefficient

Fuel salt temperature coefficient (FSTC) is a cumulative effect of fuel salt Doppler coefficient and fuel salt density coefficient, which can also be divided into four parts, namely fast fission coefficient, resonance escape coefficient, thermal reproduction coefficient, and thermal utilization coefficient caused by the fuel salt temperature effect. Figure 5 shows the variations of four reactivity coefficients that are responsible for the behavior of FSTC.

The change in fast fission factor caused by the temperature change of fuel salt, $\alpha_{\mathrm{T}}^{\varepsilon}$(salt), is a sum of fuel salt Doppler effect and fuel salt density effect. Since the contribution of the positive Doppler effect is smaller than the negative fuel salt density effect, the fast fission coefficient in FSTC is negative. The variation of fast fission coefficient in FSTC with fuel salt volume fraction and assembly size is very similar to that in fuel salt density effect, and is displayed in Figure 5 (a). When neutron spectrum hardens (or softens) due to variations in fuel salt volume fraction or assembly size, the EALF raises (or falls), the magnitude of fast fission coefficient in FSTC increases (or decreases). That is, the magnitude of fast fission coefficient in FSTC correlates positively with EALF.

The change in resonance escape probability caused by the temperature change in fuel salt, α_{T}^{p}(salt), is also a sum of fuel salt Doppler effect and fuel salt density effect. For most combinations of fuel salt volume fraction and assembly size, the positive resonance escape coefficient caused by the fuel salt density effect is stronger than the negative resonance escape coefficient caused by the Doppler effect, resulting in a positive resonance escape coefficient in FSTC. However, for an assembly with a smaller assembly size (e.g., L=3 cm) and a smaller fuel salt volume fraction (e.g., VF$<$10%), the positive resonance escape coefficient caused by the fuel salt density effect is weaker than the negative resonance escape coefficient caused by the Doppler effect, resulting in a relatively weaker negative resonance escape coefficient in FSTC. From Figure 5 (b), at a constant assembly size, the negative resonance escape coefficient in FSTC becomes weaker and turns to a more stronger positive feedback with increasing fuel salt volume fraction. This is mainly due to a gradual increased positive resonance escape coefficient caused by the fuel salt density effect. The magnitude of resonance escape coefficient in FSTC with a fixed fuel salt volume fraction is divided into two main regions by the change of assembly size. In the over-moderated region, as assembly size increases, the resonance escape coefficient in FSTC shifts from weaker negative feedback to stronger positive feedback due to a weakening negative resonance escape coefficient caused by the Doppler effect. In the under-moderated region, a decreasing positive res-

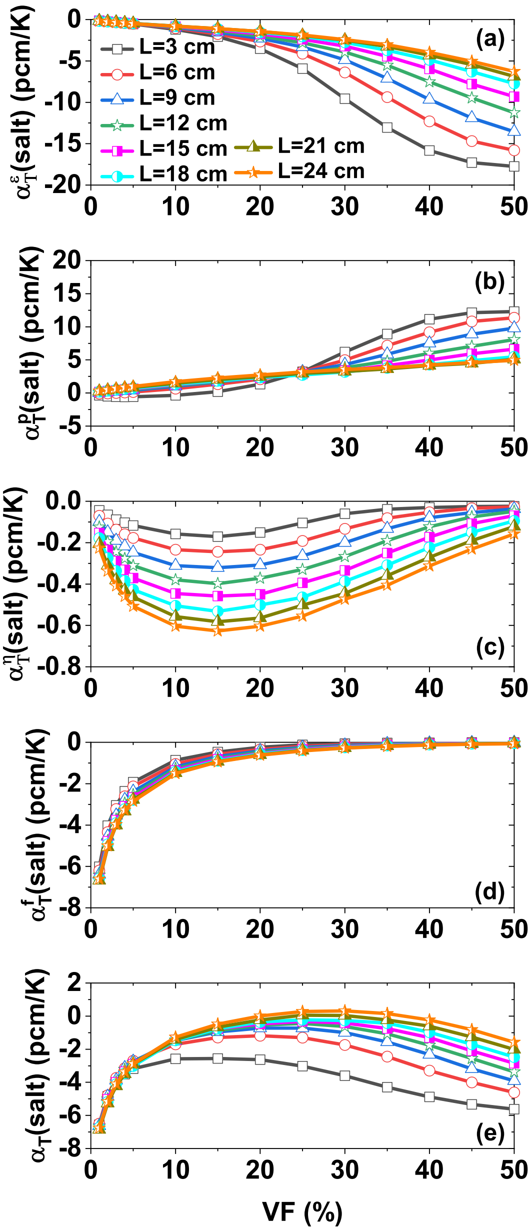

Fig. 5. Variations of different reactivity coefficients caused by the fuel salt temperature effect as function of fuel salt volume fraction and assembly size. (a) $\alpha_{\rm T}^{\varepsilon}$(salt): fast fission coefficient in FSTC; (b) $\alpha_{\rm T}^{p}$(salt): resonance escape coefficient in FSTC; (c) $\alpha_{\rm T}^{\eta}$(salt): thermal reproduction coefficient in FSTC; (d) $\alpha_{\rm T}^{f}$(salt): thermal utilization coefficient in FSTC; and (e) $\alpha_{\rm T}$(salt): FSTC.

onance escape coefficient caused by the fuel salt density effect causes the positive resonance escape coefficient in FSTC to gradually decrease with increasing assembly size. In general, the larger the EALF, the greater the possibility of a positive resonance escape coefficient in FSTC and the stronger the positive resonance escape coefficient in FSTC.

The thermal reproduction coefficient in FSTC is also a sum of fuel salt Doppler effect and fuel salt density effect. Because the magnitude of thermal reproduction coefficient caused by the fuel salt density effect is very small, the feedback and the magnitude of thermal reproduction coefficient in FSTC are primarily determined by the Doppler effect. The thermal reproduction coefficient in FSTC, $\alpha_{\rm T}^{\eta}$(salt), is a negative feedback. As seen from Figure 5 (c), the magnitude of thermal reproduction coefficient in FSTC increases first and then decreases as fuel salt volume fraction increases, and shows a monotonic increasing tendency as assembly size increases.

The thermal utilization coefficient in FSTC is a product of fuel salt Doppler effect and fuel salt density effect. Because both the thermal utilization coefficient caused by the Doppler effect and that caused by the fuel salt density effect are negative, the thermal utilization coefficient in FSTC, $\alpha_{\rm T}^{f}$(salt), is as well. From Figure 5 (d), at a constant assembly size, the magnitude of thermal utilization coefficient in FSTC decreases, owing primarily to a decrease in thermal utilization coefficient caused by the fuel salt density effect as fuel salt volume fraction increases while fuel salt channel spacing decreases. For a constant fuel salt volume fraction, the magnitude of thermal utilization coefficient in FSTC increases slightly due to a slightly increased thermal utilization coefficient caused by the Doppler effect, with an increase in assembly size corresponding to a larger fuel salt channel spacing. In short, the negative thermal utilization coefficient in FSTC is positively correlated with fuel salt channel spacing. The larger the fuel salt channel spacing, the stronger the negative thermal utilization coefficient in FSTC.

Figure 5 (e) displays the change in FSTC with fuel salt volume fraction and assembly size. In the over-moderated region, the feedback and the magnitude of FSTC are primarily determined by the thermal utilization coefficient, and FSTC is always negative. The magnitude of FSTC decreases as fuel salt volume fraction increases, and there is very little difference in magnitudes between different assembly sizes. In the under-moderated region, the feedback of FSTC, mainly due to fast fission coefficient, resonance escape coefficient, and thermal utilization coefficient, could be negative or positive. In this case, as fuel salt volume fraction increases, the negative FSTC decreases first due to a gradual weakening negative thermal utilization coefficient, and then increases due to the enhancement rate of fast fission coefficient being faster than that of resonance escape coefficient. Furthermore, the magnitude of FSTC declines with increasing assembly size, owing primarily to a decreasing negative fast fission coefficient. When the magnitude of positive resonance escape coefficient is larger than the magnitude of negative fast fission coefficient, FSTC presents a possibility of positive feedback especially when assembly size is greater than or equal to 21 cm. It can be concluded that the variation of FSTC with fuel salt volume fraction is primarily caused by the fuel salt density effect, whereas the variation of FSTC with assembly size is primarily caused by the fuel salt Doppler effect.

E. Moderator temperature coefficient

As graphite moderator temperature rises, the excitation of target nuclei (graphite nuclei) becomes more easily activated,

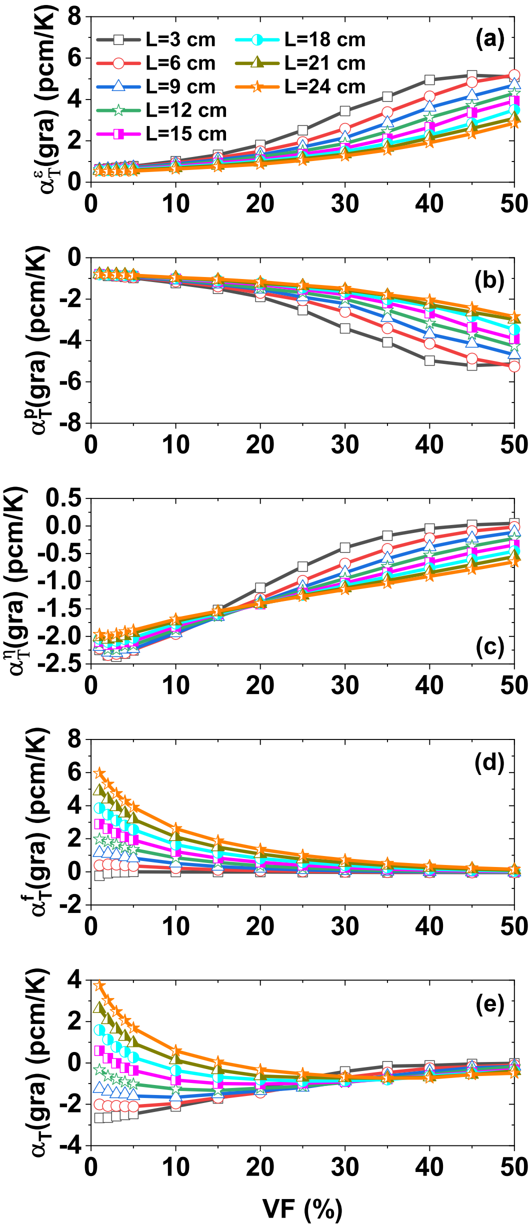

Fig. 6. Variations of different reactivity coefficients caused by the graphite moderator temperature effect as function of fuel salt volume fraction and assembly size. (a) α_T^ε(gra): fast fission coefficient in MTC; (b) α_T^p(gra): resonance escape coefficient in MTC; (c) α_T^η(gra): thermal reproduction coefficient in MTC; (d) α_T^f(gra): thermal utilization coefficient in MTC; and (e) α_T(gra): MTC.

the non-elastic scattering cross section of target nuclei becomes larger, neutrons are more likely to obtain the sound energy of the scattered target nuclei, neutron spectrum moves toward the region where neutron energy is high. And a hardener neutron spectrum is revealed. The graphite moderator temperature coefficient (MTC) can also be divided into four parts, fast fission coefficient, resonance escape coefficient, thermal reproduction coefficient, and thermal utilization coefficient, which are caused by the graphite temperature effect. Figure 6 depicts the variations of MTC and its four reactivity coefficients as a function of fuel salt volume fraction and assembly size.

As graphite moderator temperature rises, neutron spectrum hardens, the fast neutron multiplication effect increases, and the fast fission factor rises. The fast fission coefficient in MTC, α_T^ε(gra), is positive. The magnitude of fast fission coefficient in MTC is primarily determined by the difference between the variation in U-235's total production and that in U-235's thermal production, and is closely related to the fuel salt channel spacing. For a fixed assembly size, as fuel salt volume fraction increases, fuel salt channel spacing decreases, neutron spectrum becomes harder and the proportion of thermal production in total production for U-235 decreases, the difference between the variation in U-235's total production and that in U-235's thermal production becomes larger, and the magnitude of fast fission coefficient in MTC increases (Figure 6 (a)). In the over-moderated region, for a constant fuel salt volume fraction, increasing assembly size results in a hardening neutron spectrum. In this case, the larger assembly size, the greater the parasitic thermal absorption of graphite, weakening the difference between the variation in U-235's total production and that in U-235's thermal production. And then, the magnitude of fast fission coefficient in MTC decreases slightly as assembly size increases. In the under-moderated region, when the constant fuel salt volume fraction increases by assembly size, fuel salt channel spacing increases, neutron spectrum softens, the difference between the variation in U-235's total production and that in U-235's thermal production diminishes, and the fast fission coefficient in MTC weakens. In brief, the magnitude of fast fission coefficient in MTC is inversely proportional to fuel salt channel spacing.

A hardening neutron spectrum caused by an increasing graphite temperature results in a low microscopic absorption cross section of graphite and a negative change in thermal absorption of graphite. The change in thermal absorption of fuel salt is affected by the fuel salt channel spacing. When fuel salt channel spacing is small, a hardener neutron spectrum weakens the thermal absorption of fuel salt, resulting in a negative change in thermal absorption of fuel salt, and then the sum of the thermal absorptions of fuel salt and graphite is still negative. When fuel salt channel spacing is large, the average distance traveled by neutrons between two collisions increases, allowing more neutrons to pass through the epi-thermal region and slowly transition to thermal neutrons. The change in thermal absorption of fuel salt is positive. In this case, the decrease of thermal absorption of graphite exceeds the increase of thermal absorption of fuel salt due to a larger graphite volume fraction. Hence, the sum of the thermal absorptions of fuel salt and graphite remains negative, and a negative resonance escape coefficient in MTC, α_T^p(gra), is revealed for all combinations of fuel salt volume fraction and assembly size. It can be concluded from Figure 6 (b) that the magnitude of resonance escape coefficient in MTC as a function of fuel salt volume fraction and assembly size is strongly related to the fuel salt channel spacing. If fuel salt channel spacing decreases due to a change in fuel salt volume

fraction or assembly size, the variation in thermal absorption of fuel salt gradually changes from positive to negative. It means that the net decrease in thermal absorption of fuel salt grows larger and larger. Meanwhile, the increase in thermal absorption of graphite grows larger as well. Thus, the sum of changes in thermal absorptions of fuel salt and graphite enhances the resonance escape coefficient in MTC. To sum up, the negative resonance escape coefficient in MTC is generally inversely related to the fuel salt channel spacing.

For most of the combinations of fuel salt volume fraction and assembly size, an increasing graphite temperature causes a hardening neutron spectrum and a decrease in both U-235's thermal production and U-235's thermal absorption. Although U-235's thermal production is larger than U-235's thermal absorption, the former decreases faster than the latter. The variation in U-235's thermal production decreases more than that in U-235's thermal absorption, and the thermal reproduction factor decreases, causing a negative thermal reproduction coefficient in MTC ($\alpha_{\mathrm{T}}^{\eta}$(gra)). However, there are two exceptions correspond to very large fuel salt channel spacing and very small fuel salt channel spacing. When fuel salt channel spacing is very small (e.g., L= 3 cm and VF=40%), a harder neutron spectrum causes a decrease in U-235's thermal production and U-235's thermal absorption, but because graphite is relatively thin, the probability of thermal neutron generation is reduced. The values of U-235's thermal production and U-235's thermal absorption are close, and the difference between them exceeds the difference between the decreases of U-235's thermal production and that of U-235's thermal absorption. And then, the variation in U-235's thermal production decreases less than that in U-235's thermal absorption, and thus the thermal reproduction factor decreases and a positive thermal reproduction coefficient in MTC is presented. For extremely large fuel salt channel spacing (e.g., L=24 cm and VF=1%), neutrons passing through thick graphite between two collisions with nuclear fuel have a higher chance of slowing down to thermal neutrons. U-235's thermal production and U-235's thermal absorption are increasing, but the gap between them is wider than the gap between the increment of U-235's thermal production and that of U-235's thermal absorption. The variation in U-235's thermal production increases less than that in U-235's thermal absorption, the thermal reproduction factor decreases, and a negative thermal reproduction coefficient in MTC emerges. According to the findings of MTC [12], the magnitude of thermal reproduction coefficient in MTC is inversely related to the U-235 enrichment and the EALF, mainly due to the competition between the change of thermal production and that of thermal absorption. On the one hand, as shown in Figure 2 (c) and Figure 2 (d), the required critical enrichment of U-235 decreases first and then increases while EALF increases monotonously with increasing fuel salt volume fraction at a fixed assembly size. After superimposing the two effects, the magnitude of thermal reproduction coefficient in MTC with increasing fuel salt volume fraction for a constant assembly size is as follows (Figure 6 (c)): increases slowly at first, primarily due to a decreasing U-235 enrichment, and then decreases rapidly due to an increasing U-235 enrichment and an increasing EALF, and eventually turns to a positive feedback when fuel salt channel spacing is very small. The correlation between thermal reproduction coefficient in MTC and assembly size, on the other hand, is related to the moderated regions. As assembly gets closer to the over-moderated region, both U-235 enrichment and EALF increase as assembly size increases, and the magnitude of thermal reproduction coefficient in MTC decreases. Also, as assembly gets closer to the under-moderated region, the values of U-235 enrichment and EALF decrease as assembly size increases, and the magnitude of thermal reproduction coefficient in MTC increases.

As the temperature of graphite moderator rises, neutron spectrum hardens, causing thermal absorption of graphite to fall. The fuel salt channel spacing influences the change in thermal absorption of fuel salt. The neutron spectrum effect dominates for a smaller assembly size (e.g., L=3 cm). The harder neutron spectrum reduces the thermal absorption of fuel salt, including the thermal absorptions of heavy metal and carrier salt. Because the graphite thickness for neutrons passing through between two adjacent fuel salt channels is relatively thin in this case, the decrease of thermal absorption of heavy metal is faster than that of the sum of the thermal absorptions of carrier salt and graphite, and the decrement of the variation of thermal absorption of heavy metal is higher than that of the sum of the thermal absorptions of carrier salt and graphite, and then the thermal utilization factor decreases, and thus the thermal utilization coefficient in MTC, α_{T}^{f}(gra), shows a negative feedback. For a larger assembly size (e.g., L=24 cm), the feedback of thermal utilization coefficient in MTC is divided into two cases according to the moderated regions. On the one hand, when assembly tends to the over-moderated region (e.g., L=24 cm and VF=1%), the probability of a neutron slowing to a thermal neutron increases, as does the thermal absorption of fuel salt, increasing both thermal absorption of heavy metal and that of carrier salt. Because of the relatively thicker graphite moderator, the decrease of thermal absorption of graphite is greater than the increase of thermal absorption of carrier salt in this case. The sum of thermal absorptions of carrier salt and graphite has a decreasing trend, and then the increment of the variation of thermal absorption of heavy metal and the decrement of the variation of the sum of the thermal absorptions of carrier salt and graphite make thermal utilization factor increases, and thus the thermal utilization coefficient in MTC is positive. On the other hand, when assembly tends to the under-moderated region (e.g., L=24 cm and VF=40%), a harder neutron spectrum decreases the thermal absorption of heavy metal and the sum of the thermal absorptions of carrier salt and graphite. In this case, since the thermal absorption of heavy metal is much larger than the sum of the thermal absorptions of carrier salt and graphite, the variation of thermal absorption of heavy metal is larger than the variation of thermal absorption of carrier salt and graphite, which causes a positive thermal utilization coefficient in MTC. Therefore, the thermal utilization coefficient in MTC exhibits a positive feedback for a larger fuel salt channel spacing or a negative feedback for a smaller fuel salt channel spacing. It can be seen from Figure 6 (d), as fuel salt volume fraction increases for a fixed assem-

bly size, the magnitude of thermal utilization coefficient in MTC decreases because Maxwell spectrum is no longer visible. At a constant fuel salt volume fraction, as assembly size increases, the fuel salt channel spacing increases, the graphite thickness through which fast neutrons released from fuel salt increases, and the change in thermal absorption of graphite becomes more visible. The ratio of the sum of the thermal absorptions of carrier salt and graphite to the thermal absorptions of all materials is less than 1.0 but grows larger, and then the thermal utilization coefficient in MTC changes from less negative to more positive. When combined with the preceding analysis, the thermal utilization coefficient in MTC is more negative for a smaller fuel salt channel spacing; otherwise, it is less negative or even positive.

Figure 6 (e) depicts the change in MTC with fuel salt volume fraction and assembly size. Because the fast fission coefficient and the resonance escape coefficient have opposite feedbacks but similar values, the feedback and the magnitude of MTC are primarily determined by the thermal reproduction coefficient and the thermal utilization coefficient. The feedback of MTC could be negative for an assembly with a smaller fuel salt channel spacing or positive for an assembly with a larger fuel salt channel spacing. The variation of MTC with fuel salt volume fraction can be divided into two regions: L≤12 cm and L≥15 cm. When assembly size is less than or equal to 12 cm, because the magnitude of thermal reproduction coefficient is larger than thermal utilization coefficient, MTC is negative. With an increase in fuel salt volume fraction, the magnitude of MTC first increases due to an increase in thermal reproduction coefficient, and then decreases due to the fact that the decreasing rate of thermal reproduction coefficient is faster than that of thermal utilization coefficient. When assembly size is greater than or equal to 15 cm, MTC changes from a decreasing positive feedback effect to an increasing negative feedback due to a decreasing positive thermal utilization coefficient, and then to a decreasing negative feedback due to a decreasing thermal reproduction coefficient. Additionally, the difference in MTC between different assembly sizes is primarily caused by the thermal utilization coefficient. When fuel salt volume fraction is less than or equal to 25%, the negative MTC weakens and gradually turns into stronger positive feedback as the positive thermal utilization coefficient grows stronger. When fuel salt volume fraction is larger than 25%, the negative MTC increases slightly with increasing assembly size, owing to a slightly enhanced thermal reproduction coefficient. Overall, the larger fuel salt channel spacing, the more likely MTC is to be positive.

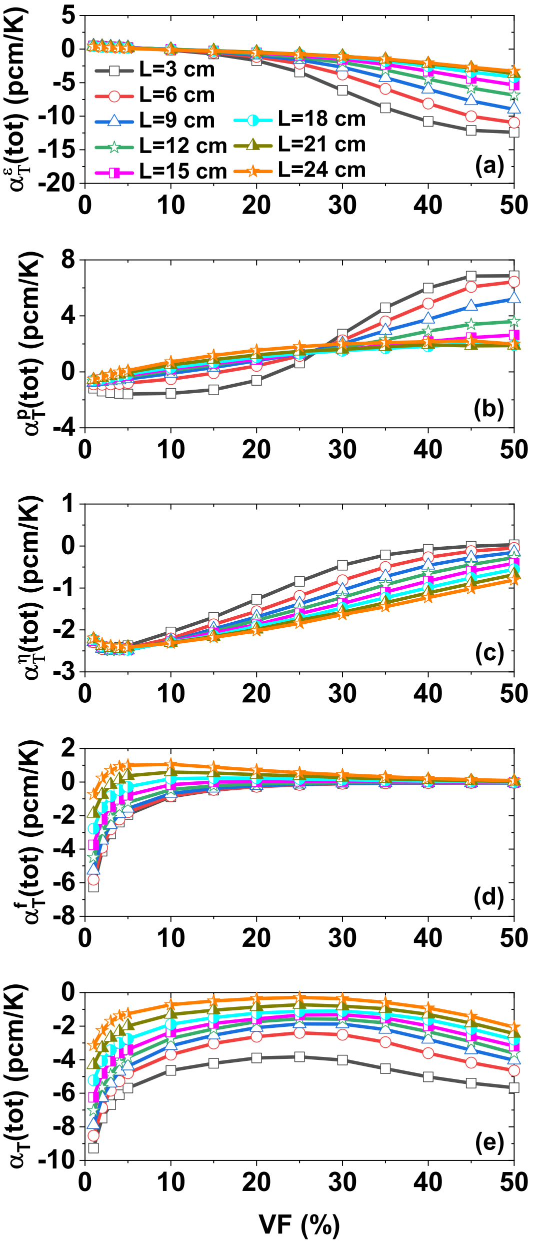

Fig. 7. Variations of different reactivity coefficients caused by the total temperature effect as function of fuel salt volume fraction and assembly size. (a) α_T^ε(tot): fast fission coefficient in TCR; (b) α_T^p(tot): resonance escape coefficient in TCR; (c) α_T^η(tot): thermal reproduction coefficient in TCR; (d) α_T^f(tot): thermal utilization coefficient in TCR; and (e) α_T(tot): TCR.

F. Temperature coefficient of reactivity

Similarly, when the temperatures of fuel salt and graphite in the assembly change, fast fission coefficient, resonance escape coefficient, thermal reproduction coefficient, and thermal utilization coefficient are contributed to the total temperature coefficient of reactivity. Their variations with fuel salt volume fraction and assembly size are shown in Figure 7.

The fast fission coefficient in TCR, α_T^ε(tot), shown in Figure 7 (a) is a sum of fuel salt temperature effect and graphite temperature effect. It can be divided into two regions by changing fuel salt volume fraction and assembly size, corresponding to the over-moderated region and the under-moderated region. In the over-moderated region, the positive fast fission coefficient in MTC is stronger than the negative fast fission coefficient in FSTC, the fast fission coefficient in TCR is positive. Due to a change in fast fission coefficient in MTC, the positive fast fission coefficient in TCR decreases

with increasing fuel salt volume fraction or increasing assembly size. In the under-moderated region, the negative fast fission coefficient in FSTC is stronger than the positive fast fission coefficient in MTC, the fast fission coefficient in TCR is negative and strengthes with increasing fuel salt volume fraction or decreasing assembly size.

The resonance escape coefficient in TCR, $\alpha_{\mathrm{T}}^{p}(\mathrm{tot})$, shown in Figure 7 (b) is also a sum of fuel salt temperature effect and graphite temperature effect. A combination of a smaller assembly size and a smaller fuel salt volume fraction increases the likelihood of resonance escape coefficient in TCR being negative, owing to a negative resonance escape coefficient in MTC. With a fixed assembly size and increasing fuel salt volume fraction, the negative resonance escape coefficient in TCR decreases gradually and then becomes an increasing positive feedback. When fuel salt volume fraction is less than 25%, the negative resonance escape coefficient in TCR gradually decreases and becomes an increasing positive feedback as assembly size increases. When fuel salt volume fraction is larger or equal to 25%, the positive resonance escape coefficient in TCR decreases with increasing assembly size.

The thermal reproduction coefficient in TCR, $\alpha_{\mathrm{T}}^{\eta}(\mathrm{tot})$, shown in Figure 7 (c) is a sum of thermal reproduction coefficients in FSTC and MTC. Because the thermal reproduction coefficient in FSTC is much weaker than that in MTC, the feedback and the magnitude of thermal reproduction coefficient in TCR are primarily determined by the latter. The feedback of thermal reproduction coefficient in TCR is negative. The variation of thermal reproduction coefficient in TCR with fuel salt volume fraction and assembly size is similar to that in MTC. When fuel salt volume fraction increases at a constant assembly size, the negative thermal reproduction coefficient in TCR increases first and then decreases. When assembly size increases for a constant fuel salt volume fraction, the thermal reproduction coefficient in TCR either weakens in the over-moderated region or strengthes in the under-moderated region.

As a sum of thermal utilization coefficients in FSTC and MTC, the thermal utilization coefficient in TCR, $\alpha_{\mathrm{T}}^{f}(\mathrm{tot})$, shown in Figure 7 (d) could be negative or positive. When assembly size is less than or equal to 12 cm, the negative thermal utilization coefficient in FSTC has a greater magnitude than the positive thermal utilization coefficient in MTC. In this case, the thermal utilization coefficient in TCR is negative, and its magnitude decreases with increasing fuel salt volume fraction, owing to a decreasing thermal utilization coefficient in FSTC. At the same time, the magnitude of thermal utilization coefficient in TCR decreases with increasing assembly size due to the fact that the thermal utilization coefficient in MTC changes from less negative to strongly positive. When assembly size is greater than or equal to 15 cm, as fuel salt volume fraction increases for a fixed assembly size, the negative thermal utilization coefficient in TCR decreases and turns into an increasing positive feedback, owing to a decreasing negative thermal utilization coefficient in FSTC, and then the positive thermal utilization coefficient in TCR decreases due to a decreasing thermal utilization coefficient in MTC. As assembly size increases for a constant fuel salt volume fraction, the negative thermal utilization coefficient in TCR weakens and then becomes a more strongly positive feedback. In a word, an assembly with a smaller fuel salt channel spacing presents higher probabilities of presenting more negative thermal utilization coefficient in TCR.

Figure 7 (e) depicts the change in TCR with fuel salt volume fraction and assembly size. The TCR is negative because the sum of the negative fast fission coefficient, the negative thermal reproduction coefficient, and the negative thermal utilization coefficient is greater than the positive resonance escape coefficient. As fuel salt volume fraction increases for a constant assembly size, the magnitude of TCR varies with fuel salt volume fraction in three cases with 5% and 25% as the cut-off points. When fuel salt volume fraction is less than or equal to 5%, the magnitude of TCR decreases rapidly, owing primarily to the rapidly decrease of the negative thermal utilization coefficient, especially that caused by the fuel salt density effect. When fuel salt volume fraction is between 5% and 25%, the magnitude of TCR decreases slowly, owing to the fact that the change rate of the sum of resonance escape coefficient, thermal reproduction coefficient, and thermal utilization coefficient is faster than that of the negative fast fission coefficient. When fuel salt volume fraction is larger than 25%, the TCR strengths slowly, owing to the fact that the growth rate of the negative fast fission coefficient is greater than that of the sum of the other three reactivity coefficients. For a constant fuel salt volume fraction, the change in TCR with assembly size is primarily due to a balance between fast fission coefficient and thermal utilization coefficient. As assembly size increases, the decrease rate of the negative fast fission coefficient is faster than that of the negative thermal utilization coefficient, so TCR weakens gradually. Finally, the magnitude of TCR decreases first and then increases with increasing fuel salt volume fraction, and it decreases monotonously with increasing assembly size. It should be noted that the contributions of fast fission coefficient, resonance escape coefficient and thermal reproduction coefficient in TCR are primarily from fuel salt density effect while the contribution of thermal utilization coefficient in TCR is mainly from fuel salt density effect and graphite temperature effect. Besides, the variation of TCR with fuel salt volume fraction mainly comes from the fuel salt density effect, whereas the variation of TCR with assembly size mainly comes from the graphite temperature effect.

IV. CONCLUSION

Based on a graphite-moderated and low-enriched uranium fueled fuel salt assembly, the four-factor formula is used to evaluate the effects of geometric parameters including fuel salt volume ratio and assembly size on TCR. When assembly temperature rises, the fuel salt Doppler effect and the graphite moderator temperature effect harden neutron spectrum, while the fuel salt density effect softens it, affecting both the feedback and the magnitude of TCR.

A positive fast fission coefficient and a negative resonance escape coefficient are observed in fuel salt Doppler coeffi-

cient and graphite moderator temperature coefficient. A negative fast fission coefficient and a positive resonance escape coefficient are revealed in fuel salt density coefficient. The feedback of thermal reproduction coefficient could be positive or negative in all reactivity coefficients. The feedback of thermal utilization coefficient in Doppler coefficient and density coefficient is negative while that in graphite moderator temperature coefficient may be negative or positive. Furthermore, Maxwell spectrum, resonant neutron spectrum, and full neutron spectrum mainly affect graphite temperature effect, fuel salt Doppler effect, and fuel salt density effect, respectively. The full neutron spectrum has the greatest influence on the changes in fast fission factor and resonance escape factor. From low to high, the magnitudes of fast fission coefficients are $\alpha_{\mathrm{T}}^{\varepsilon}$(gra), $\alpha_{\mathrm{T}}^{\varepsilon}$(dop), and $\alpha_{\mathrm{T}}^{\varepsilon}$(den). Similarly, the magnitudes of resonance escape coefficients are also α_{T}^{p}(gra), α_{T}^{p}(dop), and α_{T}^{p}(den) from low to high. Since the thermal neutron spectrum has the greatest influence on thermal reproduction factor, the magnitudes of thermal reproduction coefficients are $\alpha_{\mathrm{T}}^{\eta}$(den), $\alpha_{\mathrm{T}}^{\eta}$(dop), and $\alpha_{\mathrm{T}}^{\eta}$(gra) from low to high. The thermal utilization factor is a relatively complex variable, with magnitudes ranging from low to high for α_{T}^{f}(dop), α_{T}^{f}(gra), and α_{T}^{f}(den).

FSTC is a combined effect of fuel salt Doppler coefficient and fuel salt density coefficient. The fuel salt Doppler coefficient is always negative. The fuel salt density coefficient can be either negative in the over-moderated region due to its negative thermal utilization coefficient or positive in the under-moderated region due to its positive resonance escape coefficient. The magnitude of FSTC decreases first and then increases as fuel salt volume fraction increases. This is primarily due to the fact that the fuel salt density coefficient shifts from decreasing negative feedback to increasing positive feedback and then decreasing positive feedback. The magnitude of FSTC decreases monotonously as assembly size increases, mainly owing to a monotonously decreasing Doppler coefficient.

MTC can be negative or positive, depending on the fuel salt channel spacing. The smaller the fuel salt channel spacing, the more likely MTC is to be negative, owing to a negative thermal reproduction coefficient. Because of a gradual weakened thermal reproduction coefficient and thermal utilization coefficient, the magnitude of MTC decreases as fuel salt volume fraction increases. As assembly size increases, MTC transitions from weakened negative feedback to enhanced positive feedback as a result of the change in thermal utilization coefficient, and when fuel salt volume fraction is relatively lower, the influence of fuel salt channel spacing on MTC is more visible.

At an assembly level, the total temperature coefficient of reactivity is negative, regardless of whether the region is over-moderated or under-moderated, which meets the safety requirements of reactor operation. The magnitude of TCR in the under-moderated region is smaller than that in the over-moderated region, and the power change rate is comparatively slower, which can be conducive to reactor safety. MTC is more likely to be negative in the under-moderated region especially for an assembly with a smaller fuel salt channel spacing. As a result, an assembly with a smaller fuel salt channel spacing in the under-moderated region is preferred to achieve a reasonable negative TCR as well as a negative MTC. The thermal-hydraulic analysis and the transient analysis are also required to assess the reasonableness of the magnitude of TCR to ensure the intrinsic safety of a liquid-fueled MSR. Future work will include, but is not limited to, the following items: friction pressure drop, heat conduction ability of graphite, consequences of abnormal reactivity introduced into, and blockage of fuel salt. In addition to geometrical parameters, fuel salt composition is another crucial factor influencing TCR for a thermal MSR, especially when fuel salt reprocessing and online refueling are equipped. To fully understand the mechanism of TCR for thermal MSR, more research is needed to address how TCR is affected by both geometric parameters and fuel salt composition.

[1] V. I. Victor, Molten Salt Reactors. In: Encyclopedia Nucl Energy, **1**, 553–568 (2021). doi: 10.1016/B978-0-12-409548-9.12208-0

[2] N. Taheranpour, A. Talaei, Development of practical method using a Monte Carlo code for evaluation of optimum fuel pitch in a typical VVER-1000 core. Annals of Nuclear Energy, **54**, 129–133 (2013). doi: 10.1016/j.anucene.2012.10.029

[3] A. Rykhlevskii, J. W. Bae, K. D. Huff, Modeling and simulation of online reprocessing in the thorium-fueled molten salt breeder reactor. Annals of Nuclear Energy, **128**, 366–379 (2019). doi: 10.1016/j.anucene.2019.01.030

[4] G. C. Li, P. Cong, C. G. Yu, *et al.*, Optimization of Th-U fuel breeding based on a single-fluid double-zone thorium molten salt reactor. Progress in Nuclear Energy, **108**, 144–151 (2018). doi: 0.1016/j.pnucene.2018.04.017

[5] J. H. Wu, J. G. Chen, X. Z. Kang, *et al.*, A novel concept for a molten salt reactor moderated by heavy water. Annals of Nuclear Energy, **132**, 391–403 (2019). doi: 10.1016/j.anucene.2019.04.043

[6] L. Mathieu, D. Heuer, R. Brissot, *et al.*, The Thorium Molten Salt Reactor: Moving on from the MSBR. Progress in Nuclear Energy, **48**(7), 664–679 (2006). doi: 10.1016/j.pnucene.2006.07.005

[7] S. Q. Jaradat, A. B. Alajo, Studies on the liquid fluoride thorium reactor: Comparative neutronics analysis of MCNP6 code with SRAC95 reactor analysis code based on FUJI-U3-(0). Nuclear Engineering and Design, **314**, 251–255 (2017). doi: 10.1016/j.nucengdes.2017.02.013

[8] L. Mathieu, D. Heuer, E. Merle-Lucotte, *et al.*, Possible configurations for the thorium molten salt reactor and advantages of the fast nonmoderated version. Nuclear Science and Engineering, **161**(1), 78–89 (2009). doi: 10.13182/NSE07-49

[9] J. Křepel, B. Hombourger, C. Fiorina, *et al.*, Fuel cycle advantages and dynamics features of liquid fueled MSR. Annals of nuclear energy, **64**, 380–397 (2014). doi: 10.1016/j.anucene.2013.08.007

[10] C. Y. Zou, X. Z. Cai, D. Z. Jiang, *et al*., Optimization of temperature coefficient and breeding ratio for a graphite-moderated molten salt reactor. Nuclear Engineering and Design, **281**, 114–120 (2015). doi: 10.1016/j.nucengdes.2014.11.022

[11] X. X. Li, Y. W. Ma, C.G. Yu, *et al*., Effects of fuel salt composition on fuel salt temperature coefficient(FSTC) for an under-moderated molten salt reactor(MSR). Nuclear Science and Techniques, **29**(8), 110–119 (2018). doi: 10.1007/s41365-018-0458-1

[12] X. X. Li, D. Y. Cui, Y. W. Ma, *et al*., Influence of ^{235}U enrichment on the moderator temperature coefficient of reactivity in a graphite-moderated molten salt reactor. Nuclear Science and Techniques, **30**(11), 166–176 (2019). doi: 10.1007/s41365-019-0694-z

[13] M. L. Tan, G. F. Zhu, Y. Zou, *et al*., Research on the effect of the heavy nuclei amount on the temperature reactivity coefficient in a small modular molten salt reactor. Nuclear Science and Techniques, **30**(9), 140–150 (2019). doi: 10.1007/s41365-019-0666-3

[14] B. A. Hombourger, J. Křepel, K. Mikityuk, *et al*., Parametric Lattice Study of a Graphite-Moderated Molten Salt Reactor. Journal of Nuclear Engineering and Radiation Science, **1**(1), 011009 (2015). doi: 10.1115/1.4026401

[15] C. W. Lau, C. Demaziere, H. Nylen, U. Sandberg, Improvement of LWR thermal margins by introducing thorium. Progress in Nuclear Energy, **61**, 48–56 (2012). doi: 10.1016/j.pnucene.2012.07.004

[16] X. Wang, R. Macian-Juan. Steady-state reactor physics of the dual fluid reactor concept. International Journal of Energy Research, **42**, 4313–4334 (2018). doi: 10.1002/er.4171

[17] E. E. Bende, Temperature Reactivity Effects in Pebbles of a High-Temperature Reactor Fueled with Reactor-Grade Plutonium. Nuclear Technology, **131**(3), 279–296 (2000). doi: 10.13182/NT00-A3117

[18] M. Dallas, W. Alexander, C. Ondřej, Lattice optimization for graphite moderated molten salt reactors using low-enriched uranium fuel. Annals of Nuclear Energy, **110**, 1–10 (2017). doi: 10.1016/j.anucene.2017.06.015